First-principles investigation of quantum-mechanical effects on the diffusion of hydrogen in iron and nickel

Davide Di Stefano, Matous Mrovec, and Christian Elsässer
Fraunhofer-Institut für Werkstoffmechanik IWM, Wöhlerstr. 11, 79108 Freiburg, Germany
(Dated: November 5, 2015)

The diffusion coefficients of interstitial hydrogen in bulk Fe and Ni crystals have been calculated over a wide range of temperatures employing first-principles methods based on density functional theory. Quantum-mechanical effects have been included by means of the semi-classical transition state theory and the small-polaron model of Flynn and Stoneham. Our results show that to include such effects is crucial for a quantitative simulation of H diffusion in bcc Fe even at room temperature, while in case of fcc Ni this is less important. The comparison with other theoretical approaches as well as with experimental studies emphasizes the main advantages of the present approach: it is quantitatively accurate and computationally efficient.

I. INTRODUCTION

The diffusion behavior of H atoms in host metals and alloys has been addressed for decades in scientific research and technological application. In the case of research, the H diffusion allows for the investigation of fundamental quantum-mechanical effects in crystalline materials, such as the zero-point energy (ZPE), discrete vibrational excitations, or quantum tunneling of H isotopes. From the perspective of application, the theoretical understanding of H diffusion is essential for detrimental phenomena such as hydrogen embrittlement (HE) of steels.

Various relevant mechanisms for HE have been proposed[1–5] with most of them strongly related to diffusion and trapping of H atoms in metallic host crystals. Nevertheless, a precise quantitative determination of diffusion coefficients for H in metals is still a challenging task, since measured effective diffusion coefficients depend sensitively on the specific material as well as its microstructure[1,4,6–9]. As a result, the reported experimental data for most metals are often scattered by orders of magnitude even for nominally pure bulk phases and it is difficult to interpret them with sufficient accuracy. Perhaps the most prominent example is the diffusion of H in body-centered-cubic (bcc) Fe[10]. In this case, the scatter of data has two main reasons. First, because of the very low solubility of H in bcc Fe[2], experimental diffusion measurements need to be performed on specimens containing very low amounts of H, which makes the results extremely sensitive to structural defects (e.g., point defects, dislocations, interfaces) that are inevitable even for high purity metals. Second, the interpretation of results is typically done under the assumption that H diffusion is a purely classical phenomenon, i.e., well described by an Arrhenius-like temperature dependence. However, since hydrogen is the lightest chemical element, its diffusion is affected by quantum-mechanical effects[2]. At low temperatures, H diffusion is promoted by quantum tunneling between quantized proton states of zero point energies. At high temperatures, these effects tend to disappear and a classical over-barrier jump migration becomes the dominating mechanism[2,11–13]. The presence of two distinct migration mechanisms normally leads to a non-Arrhenius-like behavior of the diffusivity.[14,15]

First-principles calculations based on density functional theory (DFT) have been used to determine the energetics associated with the migration of interstitial H atoms in crystalline metals[16–21]. However, in these calculations all atomic nuclei are treated as point-like classical particles which can lead to inaccuracies in the description of H diffusion where quantum effects are not negligible[19,22,23]. Various methodologies have been proposed to capture the non-classical treatment of diffusion, for instance, based on the path-integral (PI) method[24–28] or the small-polaron (SP) theory[11–13,29]. These approaches can yield very accurate results, but they typically require a large amount of reliable input data. To obtain these can be a rather time-consuming task for first-principles calculations. Therefore more approximate methods (e.g., tight-binding models or empirical potentials) are often employed to reduce the computational costs[26–28]. Unfortunately, these approximate methods usually do not reach the accuracy and reliability of the first-principles methods, which makes the validity of the obtained results less certain.

An alternative approach to obtain a non-classical description of diffusion is by the so-called semi-classical transition state theory (SC-TST)[30–33]. This theory has the advantage of requiring only a small amount of input data while providing an accuracy comparable to those of the PI and SP methods. The main limitation of the SC-TST is that it can be applied only to the case of a symmetric migration path, i.e., a migration path for which the two involved metastable configurations are equivalent. For the case of an asymmetric migration path, it is possible to employ a simplified version of the SP theory[13,29], that allows to keep the computational cost as low as for the SC-TST.

In this work, we apply both the SC-TST and the simplified SP model to study the diffusion of H in bcc Fe and face-centered-cubic (fcc) Ni crystals. We show that our findings agree very well with those of the computationally more demanding PI methods[26–28], and provide a consistent interpretation of available experimental data[10,34–38].

The paper is structured as follows: in Sec. II we introduce the formalisms of the SC-TST and the SP model; in Sec. III the results obtained for the Fe-H and Ni-H systems are reported; in Sec. IV the results are discussed and compared to other theoretical and experimental data; in Sec. V we summarize the major findings and present our conclusions.

II. THEORETICAL APPROACH

The diffusivity for the migration of hydrogen in a perfect metal lattice can be obtained without exploring the dynamics of the system by means of the transition state theory (TST). Following Eyring's work[39] and assuming an uncorrelated random walk, the diffusion coefficient can be written as:

$$D_{TST} = \frac{1}{6} z R^2 \Gamma = \frac{1}{6} z R^2 \frac{kT}{h} e^{-\Delta F/kT}, \tag{1}$$

where h is the Planck constant, k is the Boltzmann constant, T is the absolute temperature, z is the number of possible

equivalent jumps away from a given position, R is the jump distance, Γ is the jump rate which can be expressed as Boltzmann's factor of the free-energy difference, ΔF, corresponding to the energy barrier between the metastable transition state (top of the barrier) and the ground state (equilibrium position).

If we consider that $\Delta F = \Delta U - T\Delta S$, with ΔU and ΔS being the differences in total energy and entropy between the transition and ground states, respectively, we can write:

$$D_{TST} = \frac{kT}{h}\frac{1}{6}zR^2 e^{\Delta S/k} e^{-\Delta U/kT}. \tag{2}$$

The free energy can be calculated as $\Delta F = -kT \ln\left(\frac{Z^0}{Z^T}\right)$, where Z^T and Z^0 are the partition functions of the transition and ground states, respectively. If we use the classical expression of the partition function in harmonic and frozen-lattice approximation, the entropy contribution ΔS reads:

$$\Delta S = -k \ln\left[\frac{kT}{h}\frac{\prod_{i=1}^{2}\nu_i^S}{\prod_{i=1}^{3}\nu_i^0}\right] - k, \tag{3}$$

where ν_i^0 and ν_i^S are the vibrational frequencies of an H atom at the stable interstitial site and at the saddle point, respectively, in the host crystal. The internal energy contribution ΔU can be instead written as:

$$\Delta U = \Delta E - kT \tag{4}$$

with ΔE being the total-energy difference between the transition state and the ground state. The term $-kT$ is the difference between the sums of the vibrational kinetic and potential energies for a classical harmonic oscillator in the transition and ground states. It originates from the fact that in the transition state there is one degree of freedom less than in the stable site.[40]

If we substitute Eqs. 3 and 4 into Eq. 2, we obtain the classical expression for the diffusion coefficient:

$$D_{TST} = \frac{1}{6}zR^2 \frac{\prod_{i=1}^{3}\nu_i^0}{\prod_{i=1}^{2}\nu_i^S} e^{-\Delta E/kT} \tag{5}$$

The simplest extension of this classical expression to take into account quantum-mechanical effects is usually done by simply adding the difference in zero point energies[16,17,21,41,42], ΔZPE, corresponding to the saddle point and the stable site, to the migration energy in the exponent of Eq. 5. Such ZPE-corrected diffusivity is then expressed as:

$$D_{TST+\Delta ZPE} = \frac{1}{6}zR^2 \frac{\prod_{i=1}^{3}\nu_i^0}{\prod_{i=1}^{2}\nu_i^S} e^{-\frac{\Delta E+\Delta ZPE}{kT}} \tag{6}$$

Despite the ZPE-correction, the prefactor and the migration energy barrier in Eq. 6 remain independent of temperature, so that both Eqs. 5 and 6 can describe in fact only the classical Arrhenius-like behavior. Another problem with Eq. 6 is that the quantum-mechanical effects should disappear for high temperature, but Eq. 6 does not converge to the classical expression of Eq. 5 with increasing temperature.

In the following, we describe how the quantum-mechanical effects can be included in a more systematic way, by using either the SC-TST[30] or the SP model developed by Flynn and Stoneham[13](denoted as FS model in the following).

Quantum-mechanical effects on the diffusion of interstitial atoms can be divided into two contributions. The first contribution is due to the ZPE of the ground state of a vibrating proton or, more generally, to the presence of discrete vibrational energy levels and their occupation at finite temperatures. The second contribution is due to quantum-mechanical tunneling.

To take the quantized vibrations (qv) of H atoms into account (including the zero-point energy corrections), it is sufficient to calculate the free energy in Eq. 1 using the quantum-mechanical expressions for the partition functions instead of the classical ones. The diffusion coefficient then reads:[20,33,43]

$$D_{qv} = \frac{1}{6}zR^2 \frac{kT}{h} \frac{\prod_{i=1}^{3} 2\sinh(\frac{h\nu_i^0}{2kT})}{\prod_{i=1}^{2} 2\sinh(\frac{h\nu_i^S}{2kT})} e^{-\Delta E/kT} \tag{7}$$

This expression has the correct limits, approaching Eqs. 5 and 6 for high and low temperatures, respectively. It is useful for the following analysis to rearrange Eq. 7 into an Arrhenius-like form, in which both the prefactor and the exponential term converge to their classical limits for high temperature. This can be done in analogy to the classical case as:

$$D_{qv} = D^*_{qv}(T)\ \ e^{-\Delta E_{qv}(T)/kT} \tag{8}$$

where the temperature dependent prefactor is given as:

$$D^*_{qv}(T) = \frac{1}{6} z R^2 \frac{\prod_{i=1}^{3} \sinh\left(\frac{1}{2}u_i^0\right)}{\prod_{i=1}^{2} \sinh\left(\frac{1}{2}u_i^S\right)}\ \ \frac{e^{\sum_{i=1}^{2} \frac{1}{2}u_i^S \coth\left(\frac{1}{2}u_i^S\right)}}{e^{\sum_{i=1}^{3} \frac{1}{2}u_i^0 \coth\left(\frac{1}{2}u_i^0\right)}} \tag{9}$$

where $u_i^x = h\nu_i^x/kT$. The temperature dependent migration barrier is then expressed as:

$$\Delta E_{qv}(T) = -kT \sum_{i=i}^{3} \frac{1}{2}u_i^0 \coth\left(\frac{1}{2}u_i^0\right) + kT \sum_{i=i}^{2} \frac{1}{2}u_i^S \coth\left(\frac{1}{2}u_i^S\right) + kT \tag{10}$$

A detailed derivation of Eqs. 8, 9, and 10 is given in Appendix A. Note that $\Delta E_{qv}(T)$ is equal to $\Delta E + \Delta ZPE$ (see Eq. 6) as $T \to 0$ while for high temperature it approaches the classical migration energy barrier, ΔE.[20,33]

While the treatment of H vibrations via Eq. 7 is the same in both SC-TST and FS methods, the description of quantum tunneling is approached differently in the two approaches. Quantum tuneling in the SC-TST is considered as a correction to the diffusivity in Eq. 7. Following Fermann and Auerbach[30], the diffusion coefficient in the SC-TST can therefore be written as:

$$D_{SC-TST} = D_{qv} Q \tag{11}$$

where the tunneling correction factor, Q, is expressed as: [30]

$$Q = \frac{exp\left(\frac{\Delta E_{qv}}{kT}\right)}{1 + exp\left(2\theta_0\right)} + \frac{1}{2}\int_{-\infty}^{\theta_0} d\theta\, \mathrm{sech}^2(\theta) exp\left(\frac{h\nu_3^S \theta}{\pi kT}\right) \tag{12}$$

with $\theta_0 = (\pi \Delta E_{qv}) \,/\, \left(h\nu_3^S\right)$, $\nu_3^S = i\tilde{\nu}$ with $\tilde{\nu}$ being the imaginary vibrational frequency at the saddle point associated with the migration direction. It should be noted that in the original work[30] ΔE_{qv} is approximated as the ZPE-corrected migration energy barrier ($\Delta E + \Delta ZPE$) while in our work the physically correct, temperature-dependent expression according to Eq. 10 is used. The integral in Eq. 12 is evaluated numerically.

In an analogous way as for Eq. 7, it is also possible to rewrite Eq. 11 in an Arrhenius-like form (see Appendix A):

$$D_{SC-TST} = D_{eff}(T)^* e^{-\Delta E_{eff}(T)/kT} \tag{13}$$

with the effective migration energy, ΔE_{eff}, and the effective prefactor, D^*_{eff}, having the proper low and high temperature limits.

As already mentioned, the SC-TST is limited to symmetric transitions where the initial and final states have identical energies. This can be easily understood by noticing that this method does not take into account any information about the final state. Hence, the SC-TST will always predict the same tunneling probability, independently whether the initial and final states are equivalent or not.

In the FS model[13], the tunneling contribution is not included as a correction to the diffusion coefficient for atomic jumps over barriers, but it is considered as a distinct diffusion mechanism with its own diffusion coefficient that can be calculated using Eq. 1. The jump rate, Γ^{FS} for proton transmission between ground states at two neighboring sites, p and p', is expressed as:[13,44]

$$\Gamma^{FS} = \left(\frac{\pi}{4\hbar^2 E_c kT}\right)^{\frac{1}{2}} J_{pp'}^2 e^{-\frac{E_c}{kT}} \tag{14}$$

where $J_{pp'}$ is the tunneling matrix element and E_c is the so-called coincidence energy. To obtain properly these two quantities requires several first-principles calculations to map out the potential energy landscape of the migrating proton in the crystalline material. The Schrödinger equation for a proton in this potential can be then solved[11,12,23].

In order to keep the computational costs low we do not follow this route but instead make several approximations. The matrix element $J_{pp'}$ is calculated assuming the harmonic approximation for the proton vibrations, the frozen lattice approximation for the host metal, and the adiabatic (Born-Oppenheimer) approximation for the light proton moving in the host lattice of heavy metal atoms (i.e., the proton remains in its adiabatic ground state). Under these conditions the matrix element can be written as:

$$J_{pp'} = S\left(ZPE_{p'} + ZPE_p\right) - K \tag{15}$$

where ZPE_x is the zero point energy at site x, m is the atomic mass of a proton (or, more generally, of an H isotope), and:

$$S = \langle\tilde{\phi}_p|\tilde{\phi}_{p'}\rangle \text{ and } K = -\frac{\hbar^2}{2m}\langle\tilde{\phi}_p|\frac{d^2}{dx^2}|\tilde{\phi}_{p'}\rangle \tag{16}$$

are the overlap and kinetic-energy integrals with $|\tilde{\phi}_p\rangle$, $|\tilde{\phi}_{p'}\rangle$ being the ground-state wavefunctions for harmonic oscillators in the neighboring sites p and p'. A detailed derivation of Eq. 15 is given in Appendix B.

The remaining quantity to calculate for evaluating Eq. 14 is the coincidence energy, E_c. It is the energy required to excite the system from a configuration consisting of one occupied, self-trapped site and one unoccupied site into a configuration at which the two neighboring sites become equivalent and energetically degenerate so that the tunneling may occur[2,23]. In case of migration between two equivalent neighboring interstitial sites, E_c can be approximated by one quarter of the self-trapping energy, E_{st}[11,45], which is the energy gained by the proton due to the local lattice distortion of the host crystal. In case of hopping between non-equivalent sites, the difference between their ground state energies needs to be added to the self-trapping energy of the proton in the initial position.

Equation 14 is valid only for a temperature range low enough to assume that the proton is in its ground state and that migration is by tunneling between two ground states only, but high enough to treat the host-lattice phonon modes classically[11,12]. In order to extend the model to a range of higher temperatures, which we are interested in, we consider a superposition of the tunneling diffusivity, Eq. 14, and the over-barrier-jump diffusivity, Eq. 7[14] so that the overall diffusivity within the FS model is give as:

$$D_{FS} = D_{qv} + \frac{1}{6}zR^2\Gamma_{FS}. \tag{17}$$

Both SC-TST (Eq. 11) and FS (Eq. 17) expressions for diffusion coefficients take into account all quantum-mechanical effects for any temperature while requiring the same amount of information from DFT calculations as the simple ZPE-corrected TST (i.e., Eq. 6).

In our study, all input parameters for Eqs. 11 and 17, namely energy barriers and vibrational frequencies, were obtained by means of DFT calculations using the mixed-basis pseudopotential (MBPP) method[46–49]. A generalized gradient approximation (GGA) was employed for exchange-correlation, and spin polarization was taken into account. For the Brillouin-zone integrations in the calculation of total energies and forces, Monkhorst-Pack k-point meshes of 4x4x4 for the supercell of bcc Fe (cubic, 16 atoms) and for the supercell of fcc Ni (cubic, 32 atoms) were used. Both supercells are relatively small, nevertheless finite-size effects are negligible, as discussed below. The minimum energy path (MEP) for the migration of a proton between neighboring interstitial sites were determined using the climbing image nudge elastic band (CI-NEB) method[50]. With these computational specifications, cubic lattice parameter values of 2.87 Å and 3.53 Å were obtained for the pure bcc Fe and fcc Ni crystals, respectively, which agree with other DFT and experimental data. The atomic positions were relaxed to forces less than 10^{-3} eV/Å. The cell volume was optimized for H in its most stable interstitial position and then kept fixed in the MEP calculations of H migration.

III. RESULTS

A. Hydrogen diffusivity in α-Fe

The most stable interstitial position for dilute hydrogen in bcc iron is in the tetrahedral site (T-site)[16–18]. The optimized lattice parameter of our 16-atom Fe supercell with a single H atom is 2.91 Å, which corresponds to about

1% volume expansion with respect to pure Fe. The MEP connecting two neighboring T-sites has been determined by a CI-NEB calculation with the corresponding classical energy barrier ΔE =90 meV. This value agrees very well with the results of previous computational studies[16,17,26,27] that used larger supercells containing up to 128 Fe atoms. This comparison also verifies that the 16-atom supercell is sufficiently large to avoid any serious finite-size errors in ΔE.

The vibrational energies of H in the tetrahedral site and at the saddle-point position were calculated within the harmonic approximation and are listed in Table I. Using these values, we computed the ZPE correction, ΔZPE=0.044 eV, which is again consistent with values obtained in other theoretical investigations.[16,17]

ΔE	$h\nu_1^0$	$h\nu_2^0$	$h\nu_3^0$	$h\nu_1^S$	$h\nu_2^S$	$h\nu_3^S$	$J_{pp'}$	E_c
0.090	0.251	0.178	0.087	0.210	0.210	0.101	0.0022	0.0035

TABLE I. Classical over-barrier migration energy, ΔE, vibrational energies, $h\nu_i^x$, tunneling matrix element, $J_{pp'}$, and coincidence energies E_c (all energies are in eV) for H in Fe. The vibrational energies are calculated from the curvatures of the energy-displacement curves of an H atom in the Fe crystal (frozen-lattice approximation). There are three distinct energies at the tetrahedral site. The reference frame is such that the $h\nu_3^0$ is the energy of vibrations parallel to the $\langle 110 \rangle$ migration path while $h\nu_1^0$ and $h\nu_2^0$ are related to vibrations in two perpendicular directions.

The vibrational energies are used to calculate the diffusion coefficient for H in bcc Fe within the SC-TST according to Eq. 11 and within the FS model according to Eq. 17. The jump distance R was chosen to be the geometrical distance between two neighboring tetrahedral sites along $\langle 110 \rangle$, i.e., $R = \frac{\sqrt{2}}{4}a$, where $a = 2.91$ is the corresponding lattice parameter for the $Fe_{16}H$ supercell.

The resulting temperature dependences of the H diffusion coefficient are plotted in Fig. 1 together with those obtained from classical TST with (Eq. 6) and without (Eq. 5) the ZPE correction. Both TST dependencies have the expected Arrhenius-like behavior ($ln(D) \propto 1/T$), albeit with different slopes. The dependencies obtained using the SC-TST and the FS model are clearly non-Arhenius, both showing a strong convex bending. A good agreement between the two approaches can be seen in Fig. 1, with small differences becoming apparent only at low temperatures.

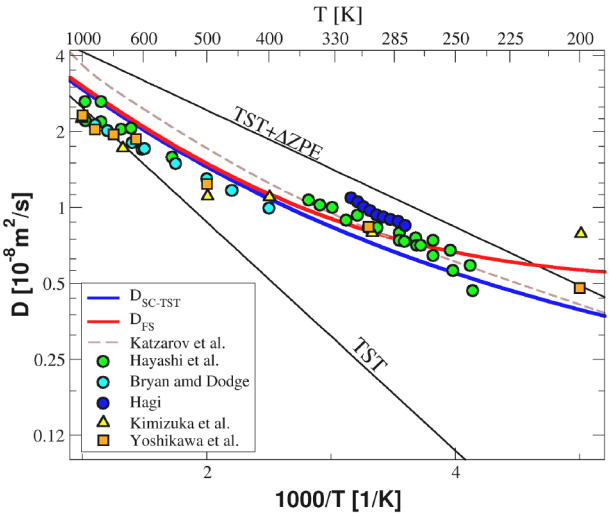

FIG. 1. Temperature dependencies of diffusion coefficients for the Fe-H system. The solid blue and red curves represent our results obtained by means of the SC-TST and FS model, respectively. The dashed brown curve corresponds to theoretical PI-method results of Katzarov et al.[26] while the triangles and the squares mark results of similar calculations obtained by Kimizuka et al.[27] and Yoshikawa et al.[28], respectively. Experimental data from[34],[51], and[52] are shown by circles. For completeness the results obtained with classical TST with and without ΔZPE correction are shown as thin black lines.

B. Hydrogen diffusivity in fcc Ni

In bulk fcc Ni, H atoms migrate between the most stable octahedral interstitial sites (O-sites) through metastable tetrahedral sites (T-sites). Consequently, the MEP consists of two jumps, one from the initial O-site to a neigboring T-site and another from this T-site to the final O-site. The first O-T jump is characterized by a much higher classical

energy barrier ($\Delta E^{O-T} = 0.37$ eV) than the second T-O jump ($\Delta E^{T-O} = 0.10$ eV). Since the O-T transition governs the H diffusion in fcc Ni, it is sufficient to consider only the ΔE^{O-T} barrier as the overall diffusion barrier. This approximation means that once the proton has overcome the first barrier to the T-site, it proceeds immediately to the final O-site. In this case, the overall jump distance corresponds to the distance between two neighboring O-sites along $\langle 110 \rangle$, i.e., $R = \frac{\sqrt{2}}{2}a$ with $a = 3.54$ Å for our $Ni_{32}H$ supercell.

A complication associated with the two-step MEP is that there exist, in principle, also two possible tunneling mechanisms. The first one is from an O-site to a T-site while the second one is directly between two neighboring O-sites. Unfortunately, in neither of these two cases it is possible to employ the SC-TST to estimate the diffusion coefficient. In the first case, the initial O-site and the final T-site are not equivalent and hence the transition cannot be treated with the SC-TST. In the second case, the direct O-O tunneling along $\langle 110 \rangle$ direction cannot be seen as a correction to the classical O-T-O over-barrier jumps along $\langle 111 \rangle$ directions since the geometrical paths are different.

The FS method is not affected by the two-step MEP and can be applied to investigate both tunneling processes independently. However, we found that both tunneling contributions are negligible (the tunneling matrix elements are less than 10^{-6}) so that the H diffusivity in fcc Ni is described accurately by Eq. 7 only. This result is shown in Fig. 2 together with the diffusivities obtained from the classical TST with and without the ZPE corrections, and experimental data. All the calculated quantities used as input data to evaluate the H diffusion coefficient in fcc Ni are listed in Table II. Note that the frequencies at the O-site and T-site are three-fold degenerate while at the saddle point they are twofold degenerate.

ΔE^{O-T}	ΔE^{O-O}	$h\nu^{O}_{1,2,3}$	$h\nu^{T}_{1,2,3}$	$h\nu^{S}_{1,2}$	$h\nu^{S}_{3}$	$J_{pp'}$	E_c^{O-O}	E_c^{O-T}
0.37	0.84[20]	0.10	0.15	0.21	0.10	$< 10^{-6}$	0.0015	$\Delta E_{qv}^{O-T}(T)$

TABLE II. Classical migration energies ΔE^x, vibrational energies $h\nu^x$, tunneling matrix element $J_{pp'}$, and coincidence energies E_c^x for H in fcc Ni (all energies are in eV).

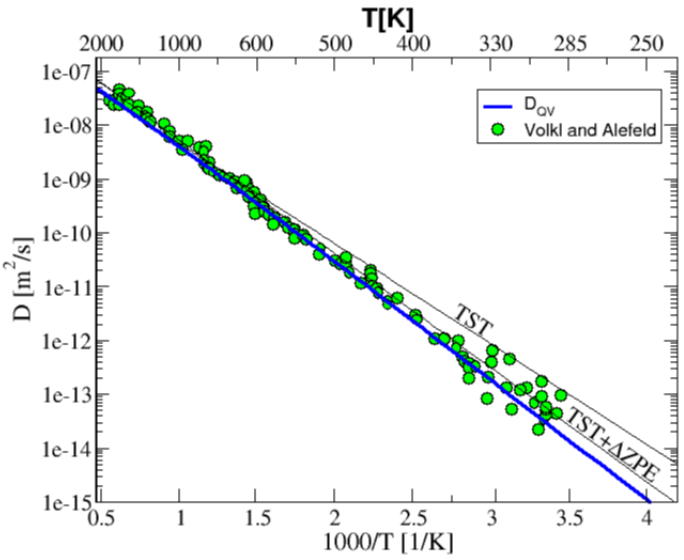

FIG. 2. Temperature dependencies of diffusion coefficients for the Ni-H system. The solid blue line represents results obtained in this study using the FS model while the results obtained using classical TST with and without ΔZPE correction are shown as thin black lines; experimental data from Ref.[53] are marked by green circles.

IV. DISCUSSION

The temperature dependencies of diffusion coefficients for H in bcc Fe obtained by the SC-TST and the FS model, shown in Fig. 1, agree well. Both models predict a clear non-Arhenius-like behavior with a strong enhancement of diffusivity at low temperatures due to quantum effects. For low temperatures, the curve obtained by means of the

SC-TST is somewhat lower than the outcome of the FS model, but the absolute differences remain rather small. For high temperatures, both curves coincide and converge to the result of classical TST.

Our results, in particular the one obtained by means of the FS model, are in a remarkably good agreement with theoretical results of Kimizuka et al.[27] and Yoshikawa et al.[28] who employed variants of the PI method. A similar study by Katzarov et al.[26] also confirms the non-Arhenius behavior, but the obtained enhancement of diffusivity at low temperatures is less pronounced.

Apart from these theoretical results, there exist many experimental investigations on H diffusion in bcc Fe[10,34–38,51,52]. In Fig. 1, we included experimental data of Hayashi et al.[34], Hagi[51], and Bryan and Dodge[52] who provided results of individual measurements. This allows a direct comparison with the theoretical results and shows again a very good agreement between theory and experiment. Unfortunately, such a direct comparison with other experimental results is not straightforward since Arrhenius-like behavior of the diffusivity is usually anticipated in experimental analyses and only temperature independent migration energy barriers and prefactors are reported after analyzing the measurements. We refer further to these quantities as 'apparent' migration energy ΔE_{app} and 'apparent' prefactor D^*_{app}. These quantities can be compared to the effective energy barrier and prefactor, ΔE_{eff} and D^*_{eff} (see Eq. 13).

The results of such an analysis for bcc Fe are presented in Fig. 3a. The temperature-dependent effective energy barrier obtained from our D_{SC-TST} curve is drawn, as a thick blue line. Corresponding effective energy barriers reported by Katzarov et al.[26] and by Kimizuka et al.[27] are also shown. The figure also contains apparent energy barriers reported by various experimental investigations, and the temperature-independent classical (dashed line labeled as TST) and ZPE-corrected (dotted line labeled as TST+ΔZPE) TST migration energies.

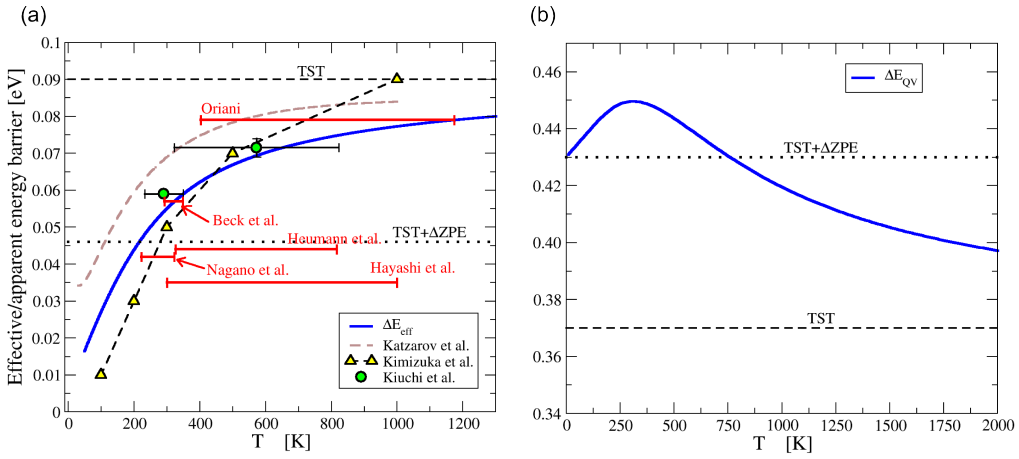

FIG. 3. (a) Comparison of effective and apparent activation energies for migration of H in bcc Fe. Experimental results from Kiuchi and McLellan[10] are reported as green circles with error bars; apparent activation energies obtained by Oriani[37], Heumann et al.[38], Beck et al.[35], Nagano et al.[36], and Hayashi et al.[34] are displayed as red bars spanning the temperature ranges in which the diffusivities have been measured. (b) Effective migration energy barrier for H in Ni. The result is compared with the classical TST migration energies with (dashed line) and without (dotted line) ΔZPE correction.

The effective migration energies from all theoretical studies shown in Fig. 3(a) exhibit the expected behavior. At high temperature they converge to the classical value of 0.09 eV, but the rate of convergence depends on the method. In the case of the SC-TST, the convergence is rather slow which is probably due to the harmonic approximation used to calculate the vibrational frequencies of the interstitial H atom. To improve the convergence, these frequency parameters perhaps need to be evaluated in a more sophisticated way[19,22,54,55].

The experimental results in Fig. 3(a) extracted from small temperature ranges show an overall good agreement with the results obtained by theory. However, this is not the case for the apparent activation energies derived from fitting over large temperature ranges. The disagreement is particularly surprising for the study by Hayashi et al.[34] since their individually measured diffusivity values agree very well with our theoretical curve of $\ln D$ vs. $1/T$ (see Fig. 1). This means that the discrepancy for the migration barrier is mainly due to the linear approximation assumed when interpreting the measured diffusivity values. This is supported by Kiuchi and McLellan[10] who carried out an extensive statistical analysis of various experimental results available from more than 40 published studies by the year 1983. Based on this analysis, they isolated two distinct temperature regimes associated with two apparent energy barriers. As shown in Fig. 3(a), these energy barriers are in good quantitative agreement with our result.

Interestingly, the ZPE-corrected energy barrier, $\Delta E + \Delta ZPE = 0.046$ eV, is within the range of values derived from the experimental data[34,36,38]. This agreement is only accidental and rather unfortunate since the ZPE correction is used widely[16,17,21,41,42] as the simplest way to include the quantum corrections. The ZPE correction is strictly correct

only at $T = 0$ K and vanishes for high temperatures. As shown in Fig. 3(a), the ZPE-corrected migration energy barrier overestimates the effective energy barrier at low temperatures (below 200 K) and underestimates it for temperatures above 400 K. The agreement with the effective energy barrier and some of the experimental estimates around room temperature is only fortuitous since the overestimated ZPE-contribution at room temperature is in fact compensated by the missing tunneling contribution. Hence, these two strong approximations apparently result in a value for the energy barrier which appears to be reasonable around room temperature.

In fcc Ni, the quantum effects do not alter the Arrhenius-like diffusion behavior over the entire temperature range considered here (see Fig. 2). The reasons are two-fold. First, the energy barrier for H migration is much higher in fcc Ni than in bcc Fe and, hence, the relative contribution of quantum corrections is much smaller. Second, the tunneling effects calculated from the FS model give no significant contribution. The transmission rates of the two possible tunneling mechanisms in Ni, the one connecting directly two neighboring octahedral sites and the other connecting the octahedral sites via an intermediate tetrahedral site, are negligibly low. For the former mechanism, this is because of the large distance between the involved sites in fcc Ni, more than two times larger than in bcc Fe. In the latter mechanism, the distance is smaller (still 50% larger than in Fe), but the tunneling probability is nullified by a too high coincidence energy in Ni, which is two orders of magnitude higher than in Fe.

In Fig. 2, the obtained diffusion coefficients (both classical and with quantum-mechanical corrections) are compared with a large number of experimental results[53]. Both classical and quantum-mechanical results show a good agreement with experimental data, but the quantum corrections do seem to provide a better agreement at low temperatures. This is corroborated by some experimental investigations[31,56] which have reported isotope effects that can be explained by considering quantum-mechanical effects.

It is interesting to notice that in the case of fcc Ni, the ΔZPE contribution increases the effective energy barrier, i.e., the diffusivity curve becomes steeper. This is in accordance with some experimental data[2] where the reported apparent migration energies tend to increase as the considered temperature increases.

Similarly to the Fe-H system, we analyzed the effective migration energy according to Eq. 10 also for the Ni-H system. As shown in Fig. 3(b), the effective migration energy shows a very different behavior than for bcc Fe. It converges to the classical migration energy for high temperatures, but it approaches the ZPE-corrected migration energy as temperature approaches 0 K. Nevertheless, it is important to keep in mind that the obtained effective energy barrier should not be taken as exact for very low temperatures because in this case other tunneling mechanisms, such as coherent tunneling[12,14,57] may become relevant. However, this low temperature regime is less relevant for practical applications.

V. CONCLUSION

Diffusion coefficients for the migration of H in bcc Fe and fcc Ni were calculated over a wide range of temperatures employing first-principles methods based on density functional theory. Quantum-mechanical effects were included by means of the semi-classical transition state theory and the small-polaron model of Flynn and Stoneham. We found that the inclusion of quantum-mechanical effects is very important for an accurate description of H migration in bcc Fe but less crucial for fcc Ni.

The obtained results were compared with those of other theoretical and experimental studies. The comparison revealed that the large scatter in the experimental results for H diffusion in bcc Fe is related to the Arrhenius-type analysis which is usually applied for the interpretation of experimental data. Hence, comparisons between theory and experiment have to be done with care and caution.

The main advantages of two presented approaches to include quantum-mechanical effects in DFT based calculations of diffusivities are their simplicity and small number of theoretical input data needed. This makes them potentially applicable to more complex situations, for instance studies of H diffusion and trapping at extended defects in polycrystalline materials[9]. Based on our results, it is possible to assess in which situations the quantum-mechanical effects are critical for an accurate description of H diffusion. For instance, for diffusion pathways between sites with significantly different energies, such as H jumps from/to trapping sites associated with crystal defects, one can expect that the tunneling effect will be negligible. However, in systems with short and symmetric diffusion pathways and moderate energy barriers, such as in bcc transition metals, quantum mechanical effects should always be considered, especially at low temperatures.

ACKNOWLEDGMENTS

This work was supported by the European Union under the Seventh Framework Programme, grant number 263335, MultiHy (Multiscale Modeling of Hydrogen Embrittlement). We thank Prof. Anthony Paxton, Dr. Ivaylo Katzarov,

and Dr. Natalia Bedoya-Martinez for helpful discussions.

Appendix A

In order to show how Eqs. 8 and 13 have been obtained, we divide and multiply Eq. 2 by e:

$$D = \frac{1}{6} z R^2 \frac{kT}{h} e^{\Delta S/k} e^1 e^{-\Delta U/kT} e^{-1}. \tag{A1}$$

Eq. A1 can then be resorted as:

$$D = \frac{1}{6} z R^2 \frac{kT}{h} e^{(\Delta S+k)/k} e^{-(\Delta U+kT)/kT} \tag{A2}$$

The above expression is an Arrhenius-like equation where the prefactor, D^*, is:

$$D^* = \frac{1}{6} z R^2 \frac{kT}{h} e^{(\Delta S+k)/k} \tag{A3}$$

and the migration energy barrier, ΔE^*, is:

$$\Delta E^* = e^{-(\Delta U+kT)/kT} \tag{A4}$$

Eqs. A3 and A4 are the most general expressions in terms of thermodynamic functions for the prefactor and the migration energy barrier and are valid both in the classical and in the quantum-mechanical cases. If now we substitute the classical expression for the entropy contribution, Eq. 3, in Eq A3, and recall that $\Delta U = \Delta E - kT$ (Eq. 4), we obtain the classical migration energy barrier and prefactor and therefore Eq. 5. If we substitute in Eqs. A3 and A4 the quantum-mechanical expressions for the total-energy and the entropy contributions[43], we obtain Eqs. 9 and 10.

Appendix B

The matrix element for tunneling of a proton between two neighboring interstitial sites p and p', $J_{pp'}$, in Eq. 14 has been calculated using Eq. 15. Here we describe concisely how to obtain this.
The Hamiltonian of a crystal containing an interstitial atom can be written as[13]:

$$\mathcal{H} = \mathcal{H}_I + \mathcal{H}_{int} + \mathcal{H}_L \tag{B1}$$

where $\mathcal{H}_I = -(\hbar/2m)\nabla^2$ is the kinetic energy of the interstitial, $\mathcal{H}_L$ is the perfect lattice Hamiltonian of the crystal, and $\mathcal{H}_{int}$ in the interaction energy between the interstitial and the lattice. This last term can be written as the sum of contributions from different interstitial sites, p:

$$\mathcal{H}_{int} = \sum_p \mathcal{H}^p_{int} \tag{B2}$$

Employing twice the Born-Oppenheimer approximation, first between the electrons and the nuclei and second between the lighter interstitial proton and the heavier lattice nuclei, it is possible to separate the eigenfunctions of $\mathcal{H}$ into products of the eigenstates of $\mathcal{H}_L$ and the eigenstates, $\tilde{\phi}_p$, of the Hamiltonian terms that act on a proton at a particular site p:

$$\left(\mathcal{H}^p_{int} + \mathcal{H}_I\right) \tilde{\phi}_p = E_p \tilde{\phi}_p \tag{B3}$$

where E_p is the energy of the proton at the site p. Within the harmonic approximation, the eigenfunction $\tilde{\phi}_p$ is the ground-state wavefunction for the harmonic oscillator centered at the site p which can be written as:

$$\tilde{\phi}_p = \left(\frac{\alpha_x\alpha_y\alpha_z}{\pi^3}\right)^{(1/4)} e^{-\frac{\alpha_x}{2}x^2-\frac{\alpha_y}{2}y^2-\frac{\alpha_z}{2}z^2} \tag{B4}$$

For a second harmonic oscillator centered at the neighboring site p', the ground-state wavefunction is:

$$\tilde{\phi}_p = \left(\frac{\alpha_x\alpha_y\alpha_z}{\pi^3}\right)^{(1/4)} e^{-\frac{\alpha_x}{2}(x+R)^2-\frac{\alpha_y}{2}y^2-\frac{\alpha_z}{2}z^2} \tag{B5}$$

where $\hat{x}$ is the direction connecting the sites p and p' separated by the distance R, $\alpha_j = \frac{m\omega_j}{\hbar}$, being ω_j the angular frequency of the proton associated with the vibrating direction $\hat{j}$.
If we consider the tunneling between two states only, the tunneling matrix element, $J_{pp'}$, can be calculated as the matrix element between the ground state of the two harmonic oscillators centered at two neighboring interstitial sites, as:

$$J_{pp'} = \langle\tilde{\phi}_p|\mathcal{H}_{int}+\mathcal{H}_I|\tilde{\phi}_{p'}\rangle \tag{B6}$$

By adding and subtracting $\langle\tilde{\phi}_p|\mathcal{H}_I|\tilde{\phi}_{p'}\rangle$, we obtain:

$$J_{pp'} = \langle\tilde{\phi}_p|\mathcal{H}^p_{int}+\mathcal{H}_I|\tilde{\phi}_{p'}\rangle + \langle\tilde{\phi}_p|\mathcal{H}^{p'}_{int}+\mathcal{H}_I)|\tilde{\phi}_{p'}\rangle - \langle\tilde{\phi}_p|\mathcal{H}_I|\tilde{\phi}_{p'}\rangle \tag{B7}$$

Using Eqs. B3, B4, and B5, and recognizing that the energies E_p are the zero point energies of the H at the sites, p and p', ZPE_p and ZPE'_p, from Eq. B7 the Eq. 15 is obtained.
Notice that, by inserting a harmonic-oscillator wavefunction in each of the two neighboring sites we mimic the situation in which the proton is delocalized between these two sites. Implicitly, this means that the probability to find a proton is non-zero in two sites only. Although we think that this condition is not particularly restrictive in the temperature range considered, it can became critical for much lower temperature or even lighter H isotopes like muons.[2,57]

[1] S. M. Myers, M. I. Baskes, H. K. Birnbaum, J. W. Corbett, G. G. DeLeo, S. K. Estreicher, E. E. Haller, P. Jena, N. M. Johnson, R. Kirchheim, S. J. Pearton, and M. J. Stavola, Rev. Mod. Phys. **64**, 559 (1992).
[2] Y. Fukai, *The Metal-Hydrogen System* (Springer, 2004).
[3] A. Pundt and R. Kirchheim, Annu. Rev. Mater. Res. **36**, 555 (2006).
[4] I. M. Robertson, H. Birnbaum, and P. Sofronis, in *Dislocations in solids 15*, edited by L. Kubin and J. P. Hirth (North-Holland Elsevier, 1978) Chap. 88.
[5] S. Lynch, Corros. Rev. **30**, 105 (2012).
[6] A. Oudriss, J. Creus, J. Bouhattate, C. Savall, B. Peraudeau, and X. Feaugas, Scr. Mater. **66**, 37 (2012).
[7] E. Legrand, J. Bouhattate, X. Feaugas, S. Touzain, H. Garmestani, M. Khaleel, and D. Li, Comput. Mater. Sci. **71**, 1 (2013).
[8] S. Jothi, T. Croft, and S. Brown, Int. J. Hydrogen Energy **40**, 2882 (2015).
[9] D. Di Stefano, M. Mrovec, and C. Elsässer, Acta Mater. **98**, 306312 (2015).
[10] K. Kiuchi and R. B. McLellan, Acta Metall. **31**, 961 (1983).
[11] P. Sundell and G. Wahnström, Phys. Rev. B **70**, 224301 (2004).
[12] P. Sundell and G. Wahnström, Phys. Rev. Lett. **92**, 155901 (2004).
[13] C. P. Flynn and A. M. Stoneham, Phys. Rev. B **1**, 3966 (1970).
[14] B. R. Messer, A. Blessing, S. Dais, D. Höpfel, G. Majer, C. Schmidt, and W. Zag, Z. Phys. Chem. **119**, 61 (1986).
[15] J. R. Hulett, Q. Rev. Chem. Soc. **18**, 227 (1964).
[16] D. Jiang and E. Carter, Phys. Rev. B **70**, 064102 (2004).
[17] A. Ramasubramaniam, M. Itakura, M. Ortiz, and E. A. Carter, J. Mater. Res. **23**, 2757 (2008).
[18] J. Sanchez, J. Fullea, C. Andrade, and P. de Andres, Phys. Rev. B **78**, 014113 (2008).
[19] C. Elsässer, H. Krimmel, M. Fähnle, S. G. Louie, and C. T. Chan, J. Phys.: Condens. Matter **10**, 5131 (1998).
[20] E. Wimmer, W. Wolf, J. Sticht, P. Saxe, C. Geller, R. Najafabadi, and G. Young, Phys. Rev. B **77**, 134305 (2008).
[21] C. E. Wolverton, V. Ozoliņš, and M. Asta, Phys. Rev. B **69**, 144109 (2004).
[22] C. Elsässer, K. M. Ho, C. T. Chan, and M. Fähnle, J. Phys.: Condens. Matter **4**, 5207 (1992).

[23] H. Krimmel, L. Schimmele, C. Elsässer, and M. Fähnle, J. Phys.: Condens. Matter **6**, 7679 (1994).
[24] M. J. Gillan, Philos. Mag. A **58**, 257 (1988).
[25] G. A. Voth, J. Phys. Chem. **97**, 8365 (1993).
[26] I. H. Katzarov, D. L. Pashov, and A. T. Paxton, Phys. Rev. B **88**, 054107 (2013).
[27] H. Kimizuka, H. Mori, and S. Ogata, Phys. Rev. B **83**, 094110 (2011).
[28] T. Yoshikawa and T. Takayanagi, J. Phys. Chem. C **116**, 23113 (2012).
[29] D. Emin, M. I. Baskes, and W. D. Wilson, Phys. Rev. Lett. **42** (1979).
[30] J. T. Fermann and S. Auerbach, J. Chem. Phys. **112**, 6787 (2000).
[31] Y. Ebisuzaki, W. J. Kass, and M. O'Keeffe, J. Chem. Phys. **46**, 1373,1378 (1967).
[32] D. S. Sholl, J. Alloys Compd. **446-447**, 462 (2007).
[33] B. Bhatia and D. Sholl, Phys. Rev. B **72**, 224302 (2005).
[34] Y. Hayashi, H. Hagi, and A. Tahara, Z. Phys. Chem. **164**, 815 (1989).
[35] W. Beck, Proc. Roy. Soc. **290**, 220 (1966).
[36] M. Nagano, Y. Hayashi, N. Ohtani, M. Isshiki, and K. Igaki, Scripta Metall. **16**, 973 (1982).
[37] R. A. Oriani, Acta Metall. **18**, 147 (1970).
[38] T. H. Heumann and E. Domke, Berichte der Bunsengesellschaft für physikalische Chemie **76**, 825 (1972).
[39] H. Eyring, J. Chem. Phys. **3**, 107 (1935).
[40] N. Ashcroft and N. Mermin, *Solid State Physics*, HRW international editions (Holt, Rinehart and Winston, 1976) Chap. 22.
[41] M. G. Wardle, J. P. Goss, and P. R. Briddon, Phys. Rev. Lett. **96**, 205504 (2006).
[42] P. Kamakoti and D. S. Sholl, J. Membr. Sci. **225**, 145 (2003).
[43] M. Born and K. Huang, *Dynamical Theory of Crystal Lattices*, International series of monographs on physics (Clarendon Press, 1998) Chap. 4, pp. 166–212.
[44] A. M. Stoneham, J. Nucl. Mater. **69**, 109 (1978).
[45] H. Grabert and H. R. Schober, in *Hydrogen in Metals III*, edited by H. Wipf (Springer, 1997) Chap. 2, pp. 5–49.
[46] C. Elsässer, N. Takeuchi, K. M. Ho, C. T. Chan, P. Braun, and M. Fähnle, J. Phys.: Condens. Matter **2**, 4371 (1990).
[47] K. M. Ho, C. Elsässer, C. T. Chan, and M. Fähnle, J. Phys.: Condens. Matter **4**, 5189 (1992).
[48] B. Meyer, K. Hummler, C. Elsässer, and M. Fähnle, J. Phys.: Condens. Matter **7**, 9201 (1995).
[49] F. Lechermann, M. Fähnle, B. Meyer, and C. Elsässer, Phys. Rev. B **69**, 165116 (2004).
[50] G. Henkelman, B. P. Uberuaga, and H. Jonsson, J. Chem. Phys. **113**, 9901 (2000).
[51] H. Hagi, Mater. Trans. JIM **35**, 112 (1994).
[52] W. L. Bryan and B. F. Dodge, AIChE J. **9**, 223 (1963).
[53] J. Völkl and G. Alefeld, in *Hydrogen in Metals I*, edited by J. Völkl and G. Alefeld (Springer, 1978) Chap. 12, pp. 326–327.
[54] H. J. Tao, K. M. Ho, and X. Y. Zhu, Phys. Rev. B **34**, 8394 (1986).
[55] C. Elsässer, K. M. Ho, C. T. Chan, and M. Fähnle, Phy. Rev. B **44**, 10377 (1991).
[56] L. Katz, M. Guinan, and R. J. Borg, Phys. Rev. B **4**, 330 (1971).
[57] A. Seeger, in *Hydrogen in Metals I*, edited by J. Völkl and G. Alefeld (Springer, 1978) Chap. 13, p. 349.